Sensitivity analysis of the physical parameterizations in the WRF model on the prediction accuracy of meteorological parameters

Starchenko, Alexander, Kizhner, Lubov, Svarovsky, Artem, Prokhanov, Sergey

Alexander V. Starchenko, Lubov I. Kizhner, Artem I. Svarovsky, Sergey A. Prokhanov, "Sensitivity analysis of the physical parameterizations in the WRF model on the prediction accuracy of meteorological parameters," Proc. SPIE 11916, 27th International Symposium on Atmospheric and Ocean Optics, Atmospheric Physics, 119166C (15 December 2021); doi: 10.1117/12.2603387

SPIE.

Event: 27th International Symposium on Atmospheric and Ocean Optics, Atmospheric Physics, 2021, Moscow, Russian Federation

Sensitivity analysis of the physical parameterizations in the WRF model on the prediction accuracy of meteorological parameters

Alexander V. Starchenko[*a,b], Lubov I. Kizhner[a], Artem I. Svarovsky[a], Sergey A. Prokhanov[a]
[a]National Research Tomsk State University, 36 Lenin Ave., Tomsk, Russia 634050; [b]V.E. Zuev Institution of Atmospheric Optics SB RAS, 1 Academician Zuev Square, Tomsk, Russia 634055

ABSTRACT

Computational experiments were carried out using the WRF model version 4.2. The influence of different sets of parameterizations on the results of calculating the surface values of air temperature, wind speed and direction is considered. A set of parameterizations providing the best accuracy of numerical prediction (with a resolution of 1 km) of local meteorological characteristics for the conditions of Western Siberia, is selected. It was found that the set of parameterizations affects the simulation quality, but it is not the main aspect in ensuring prediction accuracy. To test the WRF model, the observations obtained using meteorological instruments of the JUC Atmosphere of the V.E. Zuev Institution of Atmospheric Optics SB RAS, the airfield information and measurement system of the Tomsk Airport, and the Tomsk weather station were employed.

Keywords: Numerical weather prediction, WRF, selection of parameterizations, real weather observations

1. INTRODUCTION

At present, in the development of weather forecasting technologies, it is still necessary to increase the detail and develop the physical content of models adapted to different regions, together with the widespread use of numerical meteorological predictive models differing in terms of territory, prediction period, and mathematical approaches. The prediction of weather conditions in cities, where the majority of the population, social, economic, and strategic objects are concentrated, is especially important.

Tomsk State University is working on the numerical modeling of meteorological conditions and atmospheric pollution in the Tomsk district using the models created by the Laboratory of Computational Geophysics and publicly available models. One such model is the WRF mesoscale model [1], which can be used for any territory, and, therefore, allows a choice of different parameterizations of physical processes and configuring them in accordance with specific conditions.

Earlier [2-3], using the WRF model version 3 [1], predictions of the state of the atmosphere for separate seasons and weather conditions were carried out for different parameterizations. Satisfactory results of its use in the conditions of the Siberian region were obtained and shortcomings in terms of accuracy of the prediction of individual meteorological values were identified. With the improvement of the WRF model, there is an increasing number of proposed physical parameterizations that offer more adequate consideration of atmospheric processes at the subgrid scale.

This study aims to investigate the impact of different parameterizations on the prediction accuracy and the selection of sets of parameterizations which allow getting the best results of the prediction of air temperature and wind in the area of the city of Tomsk using the WRF model of the latest version 4.2, 2018 [4]. In this paper, when evaluating the accuracy of predictions, special criteria are used to assess the quality of the model.

Modern prediction models of high spatial resolution include different variants of the representation of subgrid physical processes which differ in the depth of description of real conditions occurring in the atmosphere. The main factors complementing the basic system of equations are atmospheric turbulence, atmospheric moisture, radiation, soil, and orography. Urban areas are considered a special part of the earth's surface, which is different from other areas in terms of orography, the nature of the underlying surface, radiation, temperature and humidity, and dynamic characteristics. The city is also a source of heat generation.

*starch@math.tsu.ru; phone +7 382 2529-553; fax +7 382 2529-553; http://math.tsu.ru

27th International Symposium on Atmospheric and Ocean Optics, Atmospheric Physics, edited by Gennadii G. Matvienko, Oleg A. Romanovskii, Proc. of SPIE Vol. 11916, 119166C · © 2021 SPIE · 0277-786X · doi: 10.1117/12.2603387

A detailed description of the methods for the parameterization of subgrid processes is given in the User's Guide [4]. A fairly complete description of the physical blocks for the WRF model version 3.6.1, which can be used in other models, is given in [5]. It examines the impact of the sets of parameterizations on the accuracy of simulation for Montreal, Canada.

2. MATERIALS AND METHODS

2.1 Features of the WRF model implementation

In this paper, the influence of different sets of parameterizations of physical processes on the accuracy of calculations of meteorological conditions (air temperature at 2 m above the ground, wind speed and direction at 10 m above the ground) is studied for the Tomsk district. The calculations were carried out using the WRF model version 4.2 [4]. Based on the National Center for Environmental Prediction (NCEP) GFS 0.25 Degree Global Forecast Grids Historical Archive (ds084.1) reanalysis data, the initial and boundary meteorological characteristics and geodetic parameters on the calculated grid covering the study area were obtained using the programs of the WPS model preprocessing system.

The dimensions of the simulation area are 450x450 km (the geographic coordinates of the area center, 56.5° N, 85° E, coincide with the city center) with two nested subdomains with dimensions of 150x150 and 50x50 km (figure 1). The grid spacing for the areas is 9, 3, and 1 km, respectively. In the vertical direction, 41 calculating levels were studied. The calculations were carried out over a 24-hour time period, the acceleration time of the WRF model was 24 hours, and it was not taken into account in the analysis.

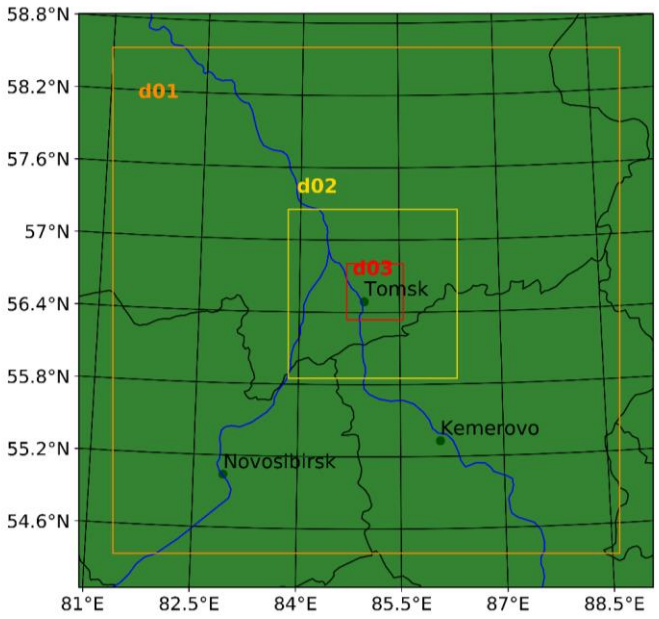

Figure 1. The simulation area.

When conducting the calculations, the following types of parameterization of subgrid processes available in the WRF model were taken into account: microphysics of moisture (mp_physics), long-wave radiation (ra_lw_physics), short-wave radiation (ra_sw_physics), surface layer (sf_sfclay_physics), land surface (sf_surface_physics), planetary boundary layer (bl_pbl_physics), cloud cover (cu_physics), urban surface (sf_urban_physics). Each type contains several variants for choosing parameterizations, from simple to complex.

Eleven combinations were used with a different choice of parameterizations of subgrid processes, and a prediction of meteorological values was made for each set. The simulation was carried out for two dates, winter (December 16, 2015) and summer (July 18, 2015). It should be noted that the selected schemes of parameterization of the microphysics of

moisture, cloud cover, and urban sublayer remained unchanged in all calculations. The choice of parameterizations aimed to find the best set for simulation of the boundary layer and its interaction with the surface layer. Therefore, different versions of turbulence models for the planetary boundary layer, the surface layer, and long-wave and short-wave radiation were considered.

2.2 Measuring system

To assess the actual state of the atmosphere, various measuring instruments located in the city and the nearest suburb of Tomsk were used. The measurements were carried out in 4 sites (figure 2).

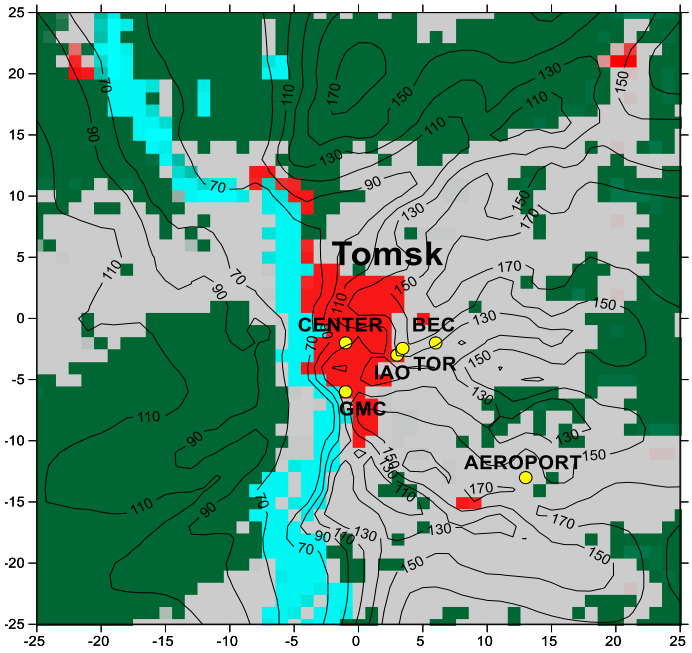

Figure 2. Terrain of the research area (terrain elevation above sea level, m) with the location of the observation sites (yellow – observation sites, blue – water, light gray – shrub or grassland, green - forest, red - urban development). The dimensions of the area are in km.

- The IAO observation site ("IAO"). The IAO observation site is located on the laboratory building roof of the IAO SB RAS (the eastern outskirts of the city of Tomsk, Akademgorodok). The MTR-5 temperature profiler [6] and the Meteo-2 ultrasonic weather station (UWS) [7] were used to measure the meteorological values. The height of these devices above the roof level is 5 m (17 m above the underlying surface level). MTR-5 carries out air temperature measurement from the placement level to the level of 1,000 m with a vertical spacing of 50 m and a time step of 5 min. The UWS measures the air temperature and relative humidity, atmospheric pressure, and wind vector components at the location point at a frequency of 10 times per second.

- Basic Experimental Complex IAO SB RAS ("BEC"). It is located in the nearest suburb of Tomsk, to the east of the city center. Natural landscape (a large clearing surrounded by woodlands) with several one-story buildings. The Meteo-2 UWS (BEK UWS) located at a height of 10 m above the underlying surface level was used to measure the meteorological values.

  The IAO observation and the Basic Experimental Complex (BEC) of the JUC Atmosphere of the V.E. Zuev Institute of Atmospheric Optics of the Siberian Branch of the RAS.

  The data averaged over the last 10 minutes of each hour were used to compare with the calculations.

- Bogashevo Airport ("Aeroport") is located in a suburb 18 km southeast of the city center. Natural landscape with several office and residential buildings. The measuring complex, AMIS-RF airfield meteorological information and measurement system, comprises standard instruments for monitoring meteorological values.

Hourly observations were used for the above sites.

- Tomsk hydrometeorological station ("GMC") is located in the southern part of the city and carries out standard meteorological observations 8 times every 24 hours.

Owing to the features of the observations, a comparison of the results of calculations of air temperature (T2) was performed for all 4 sites where meteorological observations were carried out. A comparison of calculations and observations of wind speed (Wind10) and wind direction (WDir10) was performed for 2 sites ("IAO" and "BEC").

2.3 Meteorological conditions during the experiment

On July 17-18, the territory adjacent to Tomsk was located on the western periphery of the anticyclone. The weather was clear and hot with light (1 m/s) north-east-east wind and good visibility. The extreme temperatures were 15 °C (07:00) and 29 °C (19:00). The pressure decreased from 745 to 740 mm Hg during the day. The relative humidity was 70-80% at night and 30-40% during the day.

On December 15-16, the territory was located on the axis of the ridge, the center of the anticyclone was located several hundred km to the east. The weather was cloudy with occasional showers of slight snow (from 07:00 to 18:00). The wind was light (up to 1 m/s) and south at the beginning of the period, but at the end, it changed to north-east. The visibility fluctuated from 10 km (in the case of precipitation) to 20 km. The temperature during the day was -8-9 °C, which was higher than the climatic norm without a pronounced daily course. The pressure decreased from 757 to 752 mm Hg at the end of the day. The relative humidity was 85-90%. In the surrounding area, uniform dry snow was observed in natural conditions.

2.4 The errors for different combinations of physical parameterizations.

The error analysis of the WRF model was carried out for the third internal calculation area with a size of 50x50 km. A set of generally accepted indicators for assessing the quality of a prediction of meteorological values was considered [8-10].

In this paper, the accuracy of the prediction of meteorological values was estimated by the following characteristics:

- The BIAS arithmetic mean (systematic) is a systematic overestimation or underestimation of the predictive value relative to the actual value:

$$BIAS = \frac{1}{\mathrm{N}} \sum_{i=1}^{N} \left(F_i - O_i \right) \tag{1}$$

- The MAE (mean absolute error) of the prediction which characterizes the average value of the error without taking into account its sign (with an accuracy of 0.1):

$$MAE = \frac{1}{\mathrm{N}} \sum_{i=1}^{N} \left| F_i - O_i \right| \tag{2}$$

- The RMSE (root-mean square error) of prediction is the average deviation of the value calculated using the model from the one actually observed:

$$RMSE = \sqrt{\frac{1}{N} \sum_{i=1}^{N} \left(F_i - O_i \right)^2} \tag{3}$$

- *R* correlation coefficient between predictive and actual series:

$$R = \frac{\sum_{i=1}^{N} \left(F_i - F_s \right) \left(O_i - O_s \right)}{\sqrt{\sum_{i=1}^{N} \left(F_i - F_s \right)^2} \sqrt{\sum_{i=1}^{N} \left(O_i - O_s \right)^2}} \tag{4}$$

The following notation is used in the formulas: N – the number of predictions; F_i, O_i – the predictive and actual (measured, observed) meteorological values, respectively; F_s, O_s – average value.

Obviously, such a large number of indicators allow the identification of different details in the errors of simulative predictions.

3. RESULTS

3.1 The used sets of parameterizations

Eleven calculations were carried out with different sets of parameterizations of physical subgrid processes on the considered summer (July 18, 2015) and winter (December 16, 2015) dates. The selected sets were the same for both dates. They are shown in Table 1.

Table 1. Variants of sets of physical parameterizations used in calculations.

Parameterizations	**1**	**2**	**3**	**4**	**5**	**6**		**7**		**8**	**9**	**10**	**11**
mp_physics	6	6	6	6	6	6		6		6	6	6	6
ra_lw_physics	1	1	1	1	4	14		4		4	4	4	14
ra_sw_physics	1	1	1	1	1	14		1		1	1	1	14
sf_sfclay_physics	1	2	5	2	2	2		2		10	1	1	2
sf_surface_physics	2	2	2	2	2	2		2		2	2	2	3
bl_pbl_physics	1	2	5	8	2	2		9		10	11	12	2
cu_physics	1/0/0	1/0/0	1/0/0	1/0/0	1/0/0	1/0/0		1/0/0		1/0/0	1/0/0	1/0/0	1/0/0
sf_urban_physics	0	0	0	0	0	0		0		0	0	0	0

The numbers in the table indicate the selected variant of the corresponding parameterization from those available to the model [4]. An explanation to the table is given below.

Parameterization of the microphysics of moisture (mp_physics): 6 – WSM6 scheme was used in all calculations. The WRF Single-Moment 6-class (WSM6) scheme (*mp_physics = 6*) is 6-class microphysics of moisture scheme. It considers 6 classes of atmospheric moisture states (water vapor, cloud moisture, rain moisture, ice particles, snow, sleet (hail)) [11]. This choice is based on the results of the work [2].

Parameterization of long-wave radiation (ra_lw_physics): 1; 4; 14. The Rapid Radiative Transfer Model (RRTM) scheme (*ra_lw_physics* = 1) is a scheme which uses reference tables for absorption efficiency. It takes into account several radiation bands and classes of the microphysics of moisture. To calculate the volume scattering coefficient, the following values of the concentration of gas impurities CO_2 are used: ppm, N_2O ppm, and CH_4 ppm (ppm – parts per million) [12]. The RRTMG scheme (*ra_lw_physics* = 4) is a new version of the RRTM scheme. It includes MCICA (Monte-Carlo Independent Column Approximation), the random cloud overlap method. For the main components of gas impurities $CO_2 = 379$, ppm, $N_2O = 0.319$ ppm, and $CH_4 = 1.774$ ppm are used [13]. The RRTMG-K scheme (*ra_lw_physics* = 14) is an improved version of the RRTMG scheme. For a more efficient and accurate calculation of the radiation flux, improvements were made in two aspects: the integration of the radiation transport equation over space and angle [14].

Parameterization of short-wave radiation (ra_sw_physics): 1; 14. The Dudhia scheme (*ra_sw_physics = 1*) is asimple integration through the atmosphere from top to bottom which provides a good account of the effective absorption and scattering of radiation by clouds and in clear sky [15]. The RRTMG-K scheme (ra_sw_physics = 14) is an improved version of the RRTMG scheme, added starting from the WRF model version 4.0 [14].

Parameterization of the surface layer (sf_sfclay_physics): 1, 2, 5, 10. A revised MM5 surface layer scheme using the Monin-Obukhov similarity theory [16] (*sf_sfclay_physics=11* before the WRF model version 3.6, and renamed into *sf_sfclay_physics=1* starting from the WRF model version 3.6) with the removed constraints and updated empirical

stability functions. This parameterization was added starting from the WRF model version 3.4 [17]. Starting from the WRF model version 3.7, the model's computational code is accelerated to provide synchronization similar to the old MM5 scheme. The thermal and humidity roughness lengths (or heat and moisture exchange coefficients) over the ocean were changed to the COARE 3 formula [18] starting from the WRF model version 3.7. The ETA scheme (*sf_sfclay_physics=2*) is based on the Monin-Obukhov similarity theory with the thermal roughness length by Zilitinkevich and standard similarity functions from reference tables [16]. The Mellor-Yamada-Nakanishi-Niino (MYNN) surface layer scheme (*sf_sfclay_physics=5*) is proposed for parameterizing the planetary boundary layer (PBL) of Nakanishi and Niino. It was added to the WRF model starting from version 3.1. The Total Energy – Mass Flux (TEMF) surface layer scheme (*sf_sfclay_physics=10*) is proposed for parameterization of the planetary boundary layer. It was added starting from the WRF model version 3.3 [19].

Parameterization of heat and mass transfer in soil (sf_surface_physics): 2, 3. The Noah land surface model (*sf_surface_physics=2*) is a single NCEP / NCAR scheme with numerically predicted soil temperature and humidity in four layers, partial snow cover, and frozen soil physics. Starting from the WRF model version 3.1, new modifications were added to improve the representation of processes over ice sheets and snow-covered areas [20]. The Rapid Update Cycle (RUC) land surface model (*sf_surface_physics=3*) is a parameterization which uses a layered approach to solving the balance equations, where the fluxes of atmospheric heat and mass and the fluxes of soil heat and mass are evaluated in the middle of the first atmospheric compute layer and upper soil layer, respectively, and these fluxes change the accumulation of heat and moisture in the layer covering the Earth's surface. Currently, RUC uses 9 levels in the soil with a higher resolution near the boundary with the atmosphere [4].

Parameterization of the planetary boundary layer (bl_pbl_physics): 1, 2, 5, 8, 9, 10, 11, 12. The Yonsei University scheme (*bl_pbl_physics = 1*) is a non-local K-scheme with an explicit boundary layer separation and a parabolic K-profile in an unstable mixed layer [21]. The Mellor-Yamada-Janjic scheme (*bl_pbl_physics = 2*) is an operational scheme of the ETA model which uses the one-dimensional predictive equation of the turbulent kinetic energy (TKE) with local vertical mixing [22]. Parameterization of the Mellor-Yamada-Nakanishi-Niino Level 2.5 PBL (*bl_pbl_physics = 5*) predicts the conditions for generation and dissipation of the subgrid TKE (the transition of part of the energy of ordered processes to the energy of disordered processes, and, eventually, to heat). It was added starting from the WRF model version 3.1 with a significant update in the WRF model version 3.8 [23]. The Bougeault-Lacarrère PBL scheme (*bl_pbl_physics = 8*) is a variant of parameterization with a numerical TKE prediction. It was added starting from the WRF model version 3.1. It is intended for use with the urban BEP (Building Effect Parameterization) model [24]. The UW scheme of Bretherton and Park (*bl_pbl_physics = 9*) is a numerical TKE prediction scheme taken from the CESM climate model. It was added starting from the WRF model version 3.3 [25]. The Total Energy – Mass Flux (TEMF) scheme (*bl_pbl_physics = 10*) considers the predictive variable of the subgrid total energy and shallow convection akin to mass flow. It was added starting from the WRF model version 3.3 [26]. The Shin-Hong scheme (*bl_pbl_physics = 11*) includes a scale dependence for vertical transition in the convective planetary boundary layer (PBL). Vertical mixing in a stable PBL and a free atmosphere is simulated as in the YSU scheme (*bl_pbl_physics = 1*). This scheme also diagnoses TKE and mixing length output. It was added starting from the WRF model version 3.7 [27]. The Grenier-Bretherton-McCaa scheme (*bl_pbl_physics = 12*) is a scheme for numerical TKE prediction. It was tested in the cases of cloud PBL. It was added starting from the WRF model version 3.5 [28].

Parameterization of cloud cover (Cu_physics): 1 – the Kain-Fritsch scheme for a large area, for the second and third nested areas, cloud cover was resolved explicitly. The Kain-Fritsch scheme (*cu_physics = 1*) is a subgrid scheme of deep and shallow convection which uses a mass flow approach with descending flows and a Convective Available Potential Energy (CAPE) removal time scale [29]. It is used for calculations with a horizontal grid step of >5km.

Parameterization of processes in the urban sublayer (sf_urban_physics=0) was not considered due to the absence of information on the distribution of urban land use categories (Low density residential, High density residential, Commercial) for the city of Tomsk.

3.2 The calculation results for the summer date of July 18, 2015

The results of numerical predictions of air temperature, wind speed and direction for sets of parameterizations 1-11 at two observation sites are presented in figures 3 and 4. The time here and further on is local. Good correspondence of the time course of the calculated and actual meteorological values can be noted. The air temperature is accurately predicted for three sites, with the exception of the GMC site, where there is an underestimation of the temperature during the day, especially during the daytime. This is most likely due to the more significant influence of the river in the WRF numerical

calculations. The model slightly overestimates the wind speed at the sites at night. Synchronous wind direction data indicate a good agreement between the calculated and measured values. It can be noted that Variant 11 offers a slightly worse prediction of air temperature.

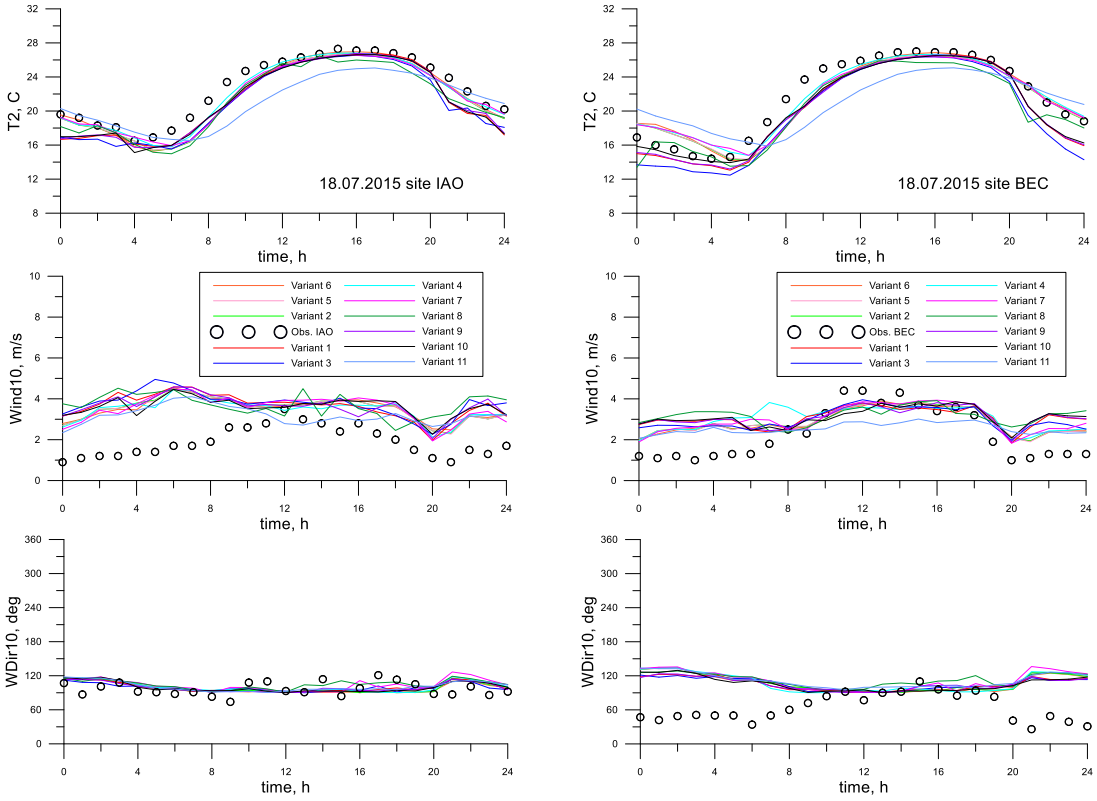

Figure 3. Calculated (lines) values of T2 surface temperature at an altitude of 2 m, Wind10 horizontal wind module, and WDir10 direction at an altitude of 10m in the selected sites (IAO and BEC). The icons indicate observations.

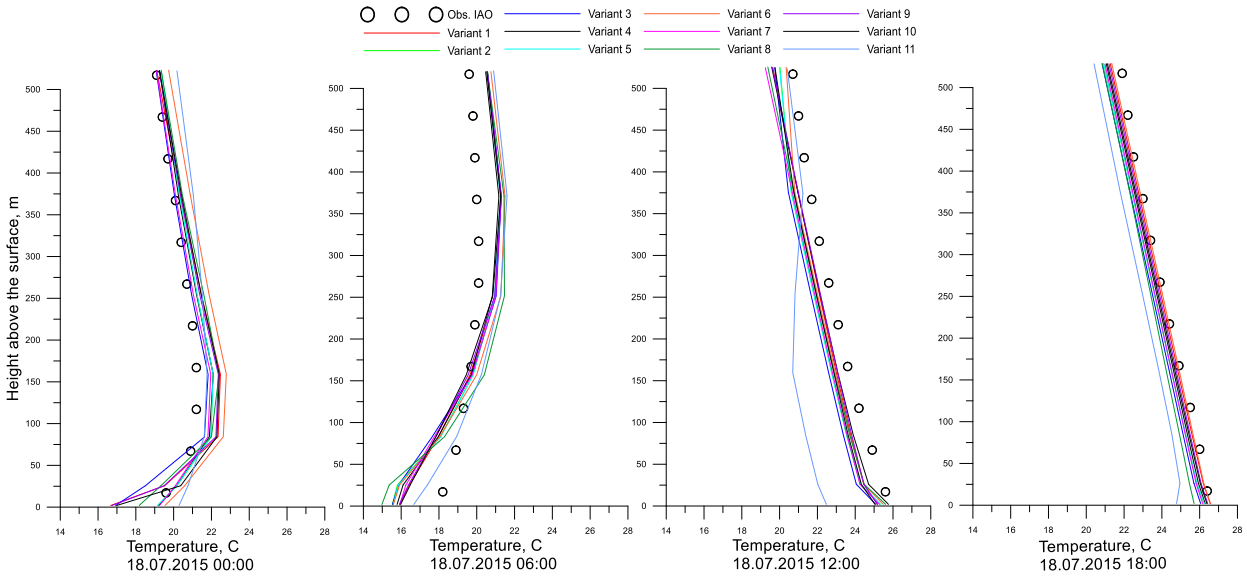

Figure 4. Predictive and actual air temperature profiles for the IAO point for the summer date of July 18, 2015. The sets of parameterizations 1-11 are used in the calculations.

Figure 4 shows the actual and calculated vertical profiles of the air temperature up to a height of 500 m at the IAO site. The data is presented for different times of day for sets 1-11. In general, the model adequately predicted the presence of an inversion layer at night (00:00) and in the morning (06:00). It can be noted that for 00:00, the best results in the entire layer are provided by Variant 2. An excellent match of the calculated and measured profiles was obtained for 18:00 using Variant 1. At other times, different sets provide similar and quite satisfactory results with the difference at individual altitudes not exceeding 2°C. It should also be noted that with the same patterns, Variant 11 is prominent because it provides the worst results.

3.3 The calculation results for the winter date of December 16, 2015

Similar calculations for December 16, 2015 are shown in figures 5 and 6. The air temperature in all observation sites (including the GMC site) was calculated with acceptable accuracy.

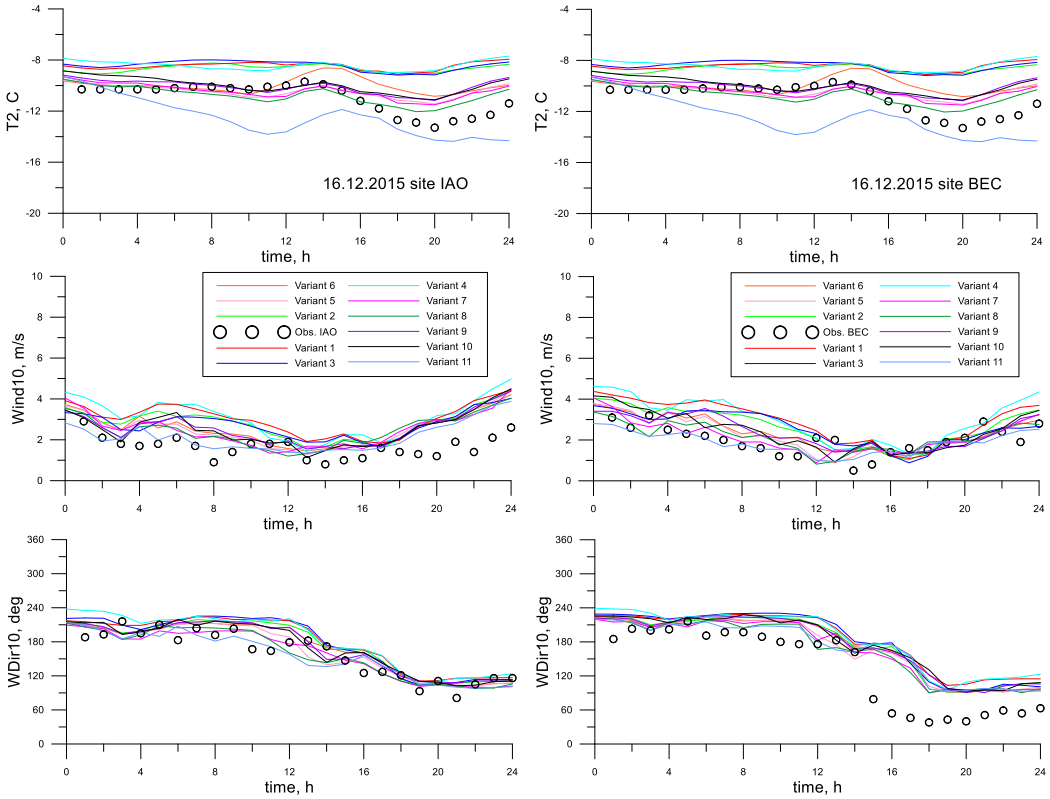

Figure 5. Calculated (lines) values of T2 surface temperature at an altitude of 2 m, Wind10 horizontal wind module, and WDir10 direction at an altitude of 10m in the selected sites (IAO and BEC). The icons indicate observations.

In general, different sets of parameterizations "work" differently in different sites. Variants 1 and 3-10 showed slightly better results on temperature. The worst result was for Variant 11, which underestimates the calculated temperature. Variant 2 tends to overestimate the temperature. As for the wind characteristics, all the variants adequately reflect the real wind and provide approximately equal values for all sites. All sets of parameterizations demonstrate an adequate representation of the vertical temperature profile, with some differences. All the variants tend to overestimate the temperature above 200 m. Variant 11 shows the worst results for the lower layer (50 m) and underestimates the temperature by up to 4°C. Such errors are observed at 06:00, 12:00 and 18:00, with the results getting better at night (00:00).

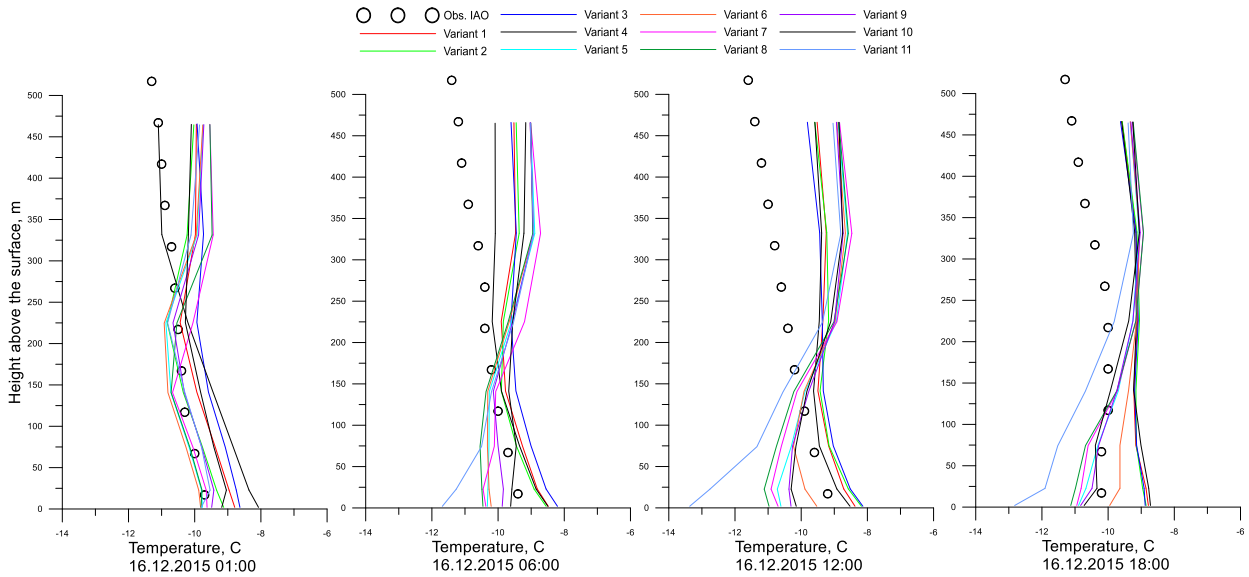

Figure 6. The predictive and actual air temperature profiles for the IAO site for the winter date of December 16, 2015.

3.4 Estimation of the model errors for different sets

To select the best sets of parameterizations of subgrid physical processes after calculating all the errors (BIAS, MAE, RMSE, R), the criteria (boundaries) were chosen that can indicate whether the result of the calculations is satisfactory or not. In general, they are consistent with the general approaches to evaluating predictions [8-10], and are more stringent in our opinion.

A justification of the criteria for air temperature and wind speed is given below. The square mean error, which strongly depends on the spread of predictive and actual meteorological values, is always the largest of the three considered errors (BIAS, MAE, RMSE). Therefore, the RMSE value <2 °C or m/s is a rather stringent criterion for evaluating the quality of the agreement between the numerically predicted and measured temperature or wind speed values. The mean absolute error (MAE) takes into account the spread of values to a lesser extent, therefore, it was taken smaller (MAE<1.5 °C or m/s). The BIAS systematic error takes into account both positive and negative differences and is even smaller in total (in absolute value). Therefore, the margin for BIAS<1 °C or m/s is also logical.

Table 2. The results of the analysis of statistical errors for the summer date (July 18, 2015).

Meteorological value, quality criteria	The site showing better/worse results	Criteria showing better/worse results	Best sets	Worst sets	Errors for the best set
T2, °C ABS(BIAS)<=1 MAE<=1.5 RMSE<=2 R>=0.90	AEROPORT, IAO, BEC/GMC	R/BIAS	4, 6 (meet all criteria) Satisfactory 7, 5, 2, 1, 9, 10 (meet the criteria, except for BIAS)	11, 8, 3	BIAS=0.72 MAE=0.75 RMSE=0.98 R=0.99
Wind10, m/s ABS(BIAS)<=1 MAE<=1.5 RMSE<=2 R>=0.7	BEC/IAO	BIAS, RMSE/R, MAE	2-7	8, 11	BIAS=-0.13 MAE=1.62 RMSE=1.72 R=0.72
WDir10, deg. MAE<45	IAO/BEC	–	1, 3, 9-10	Not expressed explicitly	BIAS=3.2 MAE=12.0 RMSE=14.3 R=0.03

Note: the suite numbers are listed in descending order of quality for the best ones and ascending quality for the worst ones.

It is proposed to take the value of MAE<45 degrees as a criterion for the horizontal wind direction because of its large instability due to the influence of many factors (roughness, relief, and stratification of the atmosphere). It means that a deviation of less than 1 rhumb from the actual wind direction is considered acceptable. The critical value of the correlation coefficient for air temperature is assumed to be 0.90, and 0.70 for wind speed, which has a greater variation in space.

Tables 2 and 3 show the results of the analysis of errors in the WRF numerical predictions for different sets of parameterizations according to these criteria for the summer (July 18, 2015) and winter (December 16, 2015) dates indicating the observation sites and the criteria to achieve the best agreement with the observations. The best and worst sets of parameterizations and the values of BIAS, MAE, RMSE, and R errors for the best set of parameterizations are shown for the winter and summer dates.

Table 3. The results of the analysis of statistical errors for the winter date (December 16, 2015).

Meteorological value, quality criteria	**The site showing better/worse results**	**Criteria showing better/worse results**	**Best sets**	**Worst sets**	**Errors for the best set**
T2, °C ABS(BIAS)<=1 MAE<=1.5 RMSE<=2 R>=0.90	GMC, AEROPORT/BEC, IAO	MAE, RMSE/R	5, 7, 9, 10	11	BIAS=0.33 MAE=0.75 RMSE=0.94 R=0.51
Wind10, m/s ABS(BIAS)<=1 MAE<=1.5 RMSE<=2 R>=0.7	BEC/IAO	MAE, RMSE/R	2, 3, 5-11	1, 4 Not expressed explicitly	BIAS 0.33 MAE=0.55 RMSE=0.67 R=0.61
WDir10, deg. MAE<45	IAO/BEC	–	2, 5-11	1, 3, 4 Not expressed explicitly	BIAS=14.2 MAE=18.1 RMSE=22.8 R=0.92

The following conclusions can be drawn from tables 2-3:

- The calculation errors (for different sets of parameterizations) differ depending on the meteorological value, season (winter or summer), site, and the selected set (suite).
- There is an obvious dependence of the model error on the selected suite of parameters (although it is not the main one).
- The latest version of the WRF model gives significantly better results than the previous models we worked with[2, 3, 30]. For the best suites, BIAS, MAE, and RMSE temperature errors do not exceed 1°C for both dates. The correlation coefficient is very high for the summer date and slightly lower for the winter date (the last column of the table).
- In terms of air temperature, the best sets on the summer date were 4 and 6, and on the winter date, those were 5, 7, 9, and 10. The worst for both dates were suites 11.
- For the selected summer and winter dates simultaneously the best temperature suites are 5, 7, 9, and 10.
- In terms of wind speed, sets 2, 3, and 5 showed the best results on the considered dates.
- In terms of wind direction, suites 9 and 10 were the best on the considered dates.
- No set was found to be the best for all the considered conditions.

Figure 7 shows the column graphs of the number of successful (satisfying the above criteria) results of comparing numerical calculations and observations depending on the parameterization number. The figure shows that for the winter date (December 16, 2015), the best sets are from 5 to 10 when the number of successfully meeting the criteria was higher than 20 for each set of parameterizations. On the summer date (July 18, 2015), the number of successfully meeting the statistical criteria of the quality of predictions is lower: 20 successful ones were achieved only for sets of parameterizations 4 and 6, slightly fewer (19) for sets 5 and 7, and 18 for set 2. The overall best sets of parameterizations (in descending order of the number of successful results) are 6, 7, 5, 9, and 10 for the two simulated cases of local weather in Tomsk.

Analyzing these results, the following recommendations can be made when choosing parameterizations of subgrid atmospheric processes in numerical modeling using the Weather Research & Forecasting system of local mesoscale meteorological processes with a resolution of 1 km for the conditions of Western Siberia. When choosing the parameterization of long-wave radiation in the atmosphere, RRTMG (ra_lw_physics=4) and RRTMG-K (ra_lw_physics=14) parameterizations give the overall best results. The Dudhia (ra_sw_physics=1) and RRTMG-K (ra_sw_physics=14) parameterizations show good results for the representation of short-wave radiation. The ETA scheme (sf_sfclay=2), which was used in sets 6,7, 2,4, and 5, is the best for parameterizing changes in the surface layer parameters. The use of the revised scheme of the MM5 model (sf_sfclay=1) based on the Monin-Obukhov similarity theory also showed good results. When parameterizing turbulent processes in the planetary boundary layer, the best agreement with observations is obtained by using the Mellor-Yamada-Janjic scheme (bl_pbl_physics=2) and the Bretherton-Park scheme (bl_pbl_physics=9). Good results were also obtained using (bl_pbl_physics=11,12) parameterizations.

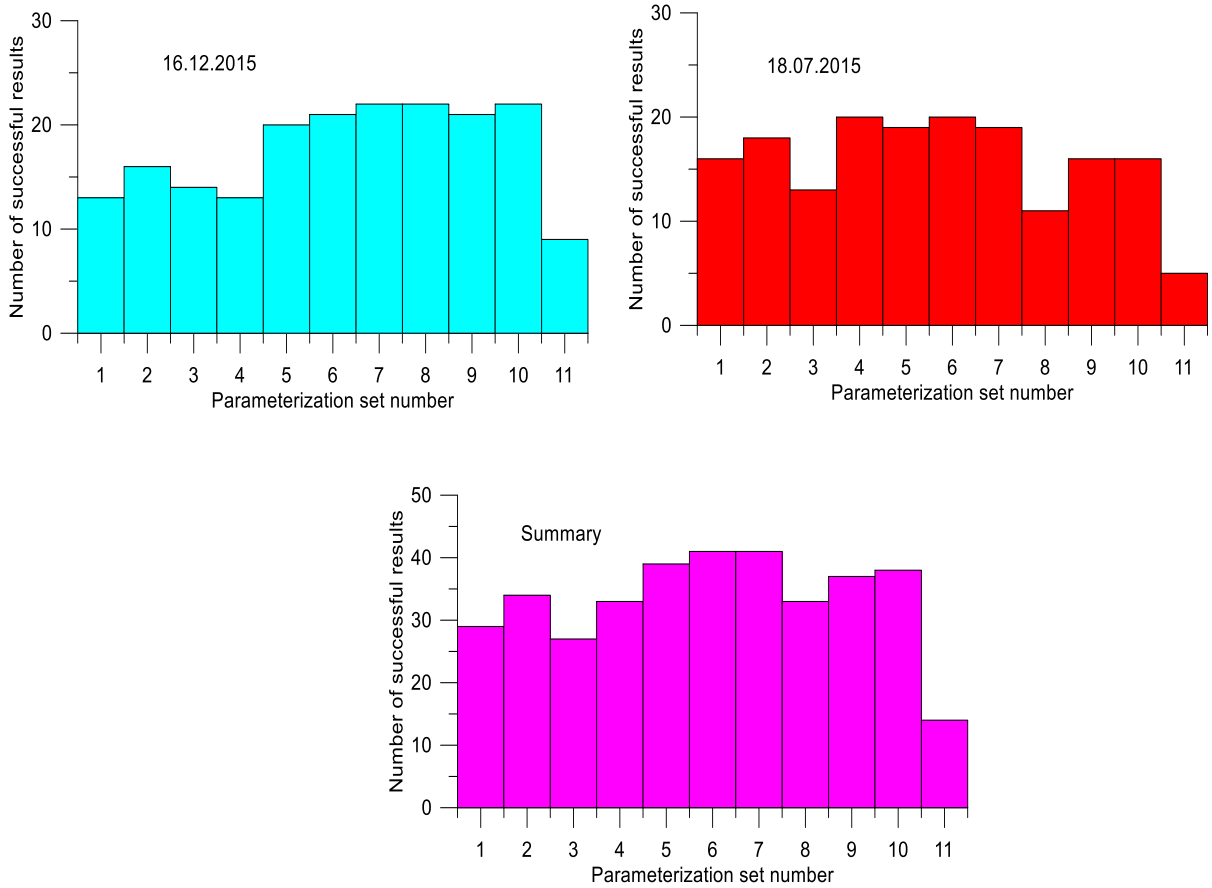

Figure 7. The number of successful results of meeting the established statistical criteria for the quality of the numerical prediction using the WRF model depending on the set of parameterizations for December 16, 2015, July 18, 2015, and overall for these two dates.

4. CONCLUSION

The paper presents some results of comparing numerical predictions with a resolution of 1 km using the WRF model version 4.2 and observational data for the conditions of Western Siberia. To test the WRF model, observations obtained using meteorological instruments of JUC Atmosphere of V.E. Zuev Institution of Atmospheric Optics SB RAS, the airfield information and measurement system of the Tomsk Airport, and the Tomsk weather station were employed. The influence of different sets of parameterizations of subgrid processes in the WRF model on the results of the numerical prediction of surface values of air temperature, wind speed and direction was considered. Based on the calculation of known statistical characteristics (BIAS, MAE, RMSE, R), criteria have been designed to evaluate the quality of agreement between the numerical predictions and observations. A set of parameterizations has been identified, which provides a more accurate numerical prediction of local meteorological conditions with a resolution of 1 km for the conditions of Western Siberia. It was found that the set of parameterizations affects the simulation quality, but it is not the main aspect in ensuring prediction accuracy.

ACKNOWLEDGEMENTS

The work was supported by the Russian Science Foundation (project no.19-71-20042).

REFERENCES

[1] Powers, J. G., Klemp, J. B., Skamarock, W. C., Davis, C. A., Dudhia, J., Gill, D. O., Coen, J. L., Gochis, D. J., Ahmadov, R., Peckham, S. E., Grell, G. A., Michalakes, J., Trahan, S., Benjamin, S. G., Alexander, C. R., Dimego, G. J., Wang, W., Schwartz, C. S., Romine, G. S., Liu, Z., Snyder, C., Chen, F., Barlage, M. J., Yu, W., Duda, M. G., "The Weather Research and Forecasting Model: Overview, System Efforts and Future Directions," Bull. Amer. Meteor. Soc. 98, 1717-1737 (2017).

[2] Kizhner, L. I., Barashkova, N. K., Akhmetshina, A. S., Bart, A. A., Starchenko, A. V., "Forecast of Precipitation in the Area of Bogashevo Airport Using the WRF Model," Atmospheric and Oceanic Optics 27, 187-194 (2014).

[3] Kizhner, L. I., Bart, A. A., Nahtigalova, D. P., "Using the numerical WRF model for the prediction of weather parameters in Tomsk region," BioClimLand: biota, climate, landscapes 1, 29-35 (2013).

[4] "ARW Version 4 Modeling System User's Guide," NCAR, https://www2.mmm.ucar.edu/wrf/users/docs/user_guide_V4/WRFUsersGuide_jan2019_tutorial.pdf.

[5] Jandaghian, Z., Touchaei, A. G., Akbari, H., "Sensitivity analysis of physical parameterizations in WRF for urban climate simulations and heat island mitigation in Montreal," Urban Climate 24, 577-599 (2018).

[6] Kadygrov, E. N., Kuznetsova, I. N., Ganshin, E. V., Gorelik, A. G., Knyazev, A. K., Miller, E. A., Nekrasov, V. V., Tochilkina, T. A. and Shaposhnikov, A. N., "Modern experience of using ground-based microwave radiometric systems for the study of atmospheric parameters," Atmospheric and Oceanic Optics 30(6), 502-508 (2017).

[7] Gladkikh, V. A., Makienko, A. E., Miller, E. A. and Odintsov, S.L., "Study of the Atmospheric Boundary Layer Parameters under Urban Conditions with Local and Remote Diagnostics Facilities. Part 2. Air Temperature and Heat Flux," Atmospheric and Oceanic Optics 23, 280-287 (2011).

[8] [RD 52.27.284-91. Guidance document. Methodical instructions. Conducting production (operational) tests of new and improved methods of hydrometeorological and heliophysical forecasts], Committee of Hydrometeorology under the Cabinet of Ministers of the USSR, Moscow (1999).

[9] [RD 52.27.724-2009. Manual for General-purpose Short-range Weather Forecasting], Federal Service for Hydrometeorology and Environmental Monitoring, Moscow, (2010).

[10] Tolstykh, M. A., Shashkin, V. V., Fadeev, R. Yu., Shlyaeva, A. V., Mizyak, V. G., Rogutov, V. S., Bogoslovskiy, N. N., Goyman, G. S., Mahnorylova, S. V., Yurova, A. Yu., [Atmosphere modelling system for seamless prediction], Triada LTD, Moscow, 166 (2017).

[11] Hong, S.-Y., Lim, J.-O., "The WRF single-moment 6-class microphysics scheme (WSM6)," J. Korean Meteor. Soc. 42, 129-151 (2006).

[12] Mlawer, E. J., Taubman, S. J., Brown, P. D., Iacono, M. J. and Clough, S. A., "Radiative transfer for inhomogeneous atmospheres: RRTM, a validated correlated-k model for the longwave," J. Geophys. Res. 102, 16663-16682 (1997).
[13] lacono, M. J., Delamere, J. S., Mlawer, E. J., Shephard, M. W., Clough, S. A. and Collins, W. D., "Radiative forcing by long-lived greenhouse gases: Calculations with the AER radiative transfer models," J. Geophys. Res. 113, D13103 (2008).
[14] Baek, S., "A revised radiation package of G-packed McICA and two-stream approximation: Performance evaluation in a global weather forecasting model," J. Adv. Model. Earth Syst. 9 (2017).
[15] Dudhia, J., "Numerical study of convection observed during the Winter Monsoon Experiment using a mesoscale two-dimensional model," J. Atmos. Sci. 46, 3077-3107 (1989).
[16] Monin, A. S. and Obukhov, A. M., "Basic laws of turbulent mixing in the surface layer of the atmosphere," Tr. Akad. Nauk SSSR Geophiz. Inst. 24(151), 163-187 (1954).
[17] Jimenez, P. A., Dudhia, J., Gonzalez-Rouco, F. J, Navarro, J., Montavez, J. P. and Garcia-Bustamante, E., "A revised scheme for the WRF surface layer formulation," Mon. Wea. Rev. 140, 898-918 (2012).
[18] Fairall, C. W., Bradley, E. F., Hare, J. E., Grachev, A. A. and Edson, J. B., "Bulk Parameterization of Air-Sea Fluxes: Updates and Verification for the COARE Algorithm," Journal of Climate 16(4), 571-591 (2003).
[19] Angevine, W. M., Jiang, H. and Mauritsen, T., "Performance of an eddy diffusivity-mass flux scheme for shallow cumulus boundary layers," Mon. Wea. Rev. 138, 2895-2912 (2010).
[20] Benjamin, S. G., Grell, G. A., Brown, J. M. and Smirnova, T. G., "Mesoscale weather prediction with the RUC hybrid isentropic-terrain-following coordinate model," Mon. Wea. Rev. 132, 473-494 (2004).
[21] Hong, S.-Y., Noh, Y., Dudhia, J., "A new vertical diffusion package with an explicit treatment of entrainment processes," Mon. Wea. Rev. 134, 2318-2341 (2006).
[22] Janjic, Z. I., "The Step-Mountain Eta Coordinate Model: Further developments of the convection, viscous sublayer, and turbulence closure schemes," Mon. Wea. Rev. 122, 927-945 (1994).
[23] Nakanishi, M. and Niino, H., "An improved Mellor-Yamada level 3 model: its numerical stability and application to a regional prediction of advecting fog," Bound. Layer Meteor. 119, 397-407 (2006).
[24] Bougeault, P., Lacarrere, P., "Parameterization of Orography-Induced Turbulence in a Mesobeta-Scale Model," Mon. Wea. Rev. 117, 1872-1890 (1989).
[25] Bretherton, C. S. and Sungsu Park, "A new moist turbulence parameterization in the Community Atmosphere Model," J. Climate 22, 3422-3448 (2009).
[26] Angevine, W. M., Jiang, H. and Mauritsen, T, "Performance of an eddy diffusivity-mass flux scheme for shallow cumulus boundary layers," Mon. Wea. Rev. 138, 2895-2912 (2010).
[27] Shin, H. H. and Hong, S.-Y. "Representation of the subgrid-scale turbulent transport in convective boundary layers at gray-zone resolutions," Mon. Wea. Rev. 143, 250-271 (2015).
[28] Herve, G. and Bretherton, C. S, "A moist PBL parameterization for large–scale models and its application to subtropical cloud–topped marine boundary layers," Mon. Wea. Rev. 129, 357-377 (2001).
[29] Kain, J. S., "The Kain–Fritsch convective parameterization: An update," J. Appl. Meteor. 43, 170-181 (2004).
[30] Starchenko, A. V., Belikov, D. A., Vrazhnov, D. A., Esaulov, A. O., "Application of MM5 and WRF mesoscale models to studies of regional atmospheric processes," Atmospheric and oceanic optics 18(5-6), 409-414 (2005).